International Journal of Nanomedicine

Dovepress
open access to scientific and medical research

Open Access Full Text Article

ORIGINAL RESEARCH

Size-dependent cellular uptake and localization profiles of silver nanoparticles

This article was published in the following Dove Press journal:
International Journal of Nanomedicine

Meiyu Wu[1,2]
Hongbo Guo[3]
Lin Liu[1,2]
Ying Liu[2,3]
Liming Xie[1,2,4]

[1]CAS Key Laboratory of Standardization and Measurement for Nanotechnology, Center for Excellence in Nanoscience, National Center for Nanoscience and Technology, Beijing 100190, People's Republic of China; [2]NCNST-NIFDC Joint Laboratory for Measurement and Evaluation of Nanomaterials in Medical Applications, National Center for Nano Science and Technology, Beijing 100190, People's Republic of China; [3]CAS Key Laboratory for Biological Effects of Nanomaterials and Nano safety, CAS Center for Excellence in Nanoscience, National Center for Nano Science and Technology, Beijing 100190, People's Republic of China; [4]University of Chinese Academy of Sciences, Beijing 100049, People's Republic of China

Purpose: Silver nanoparticles (AgNPs) have been widely applied in various fields as excellent antibacterial reagents over the past decades. Although the particle size is considered as the most crucial factor influencing cellular uptake, transportation, and accumulation behaviors, there are still many controversies regarding the correlation between size and uptake of AgNPs. In this study, size-dependent cellular uptake of AgNPs with different diameters was investigated in B16 cells.

Methods: The uptake of AgNPs was investigated by inductively coupled plasma-mass spectrometry (ICP-MS) and transmission electron microscopic (TEM) imaging in B16 cells.

Results: Twenty nanometer and 100 nm AgNPs had the lowest and highest uptake efficiency at both 12 hours and 24 hours, respectively. Smaller AgNPs crossed the plasma membrane faster with uniform distribution: 5 nm AgNPs were detected in both cytoplasm and nucleus at 0.5 hours after incubation. Larger AgNPs were extremely difficult to migrate: 100 nm AgNPs were detected in the nucleus at 12 hours after incubation. Internalization of AgNPs was directly observed, mainly within membrane-bound structures, such as intracellular vesicles and late endosomes. The uptake of all four-sized AgNPs (5 nm, 20 nm, 50 nm, 100 nm) decreased significantly after the pre-treatment with chlorpromazine hydrochloride, which can specifically inhibit the clathrin-mediated endocytosis. The internalization efficiencies of AgNPs (5 nm, 20 nm, 50 nm) were markedly reduced by methyl-β-cyclodextrin, a specific caveolin-mediated endocytosis inhibitor, whereas 5-(N-ethyl-N-isopropyl) amiloride as an inhibitor of macropinocytosis inhibited the uptake of larger sizes of AgNPs (50 nm and 100 nm).

Conclusion: The results suggest that the size of AgNPs can not only affect the efficiency of cellular uptake, but also the type of endocytosis. The clathrin-mediated endocytosis may be the most common endocytic pathway for AgNPs in B16 cells, and AgNPs at each size were likely to enter cells by a major internalization pathway.

Keywords: silver nanoparticles, size-dependence, cellular uptake, B16 cells

Introduction

With the rapid development of nanoscience and nanotechnology, products containing nanomaterials are more and more widely used in diverse areas, such as fluorescent imaging, sensing, and drug delivery.[1–3] Among the antibiotic nanomaterials, silver nanoparticles (AgNPs) were endowed to more different fields in our daily life, including textiles, sanitary articles, and cosmetics, because of their excellent broad-spectrum antimicrobial properties.[3–9] There have been many biomedical products containing AgNPs on the market to date, such as wound dressings, catheters, bone cement, and artificial cardiac valves.[10,11] With the growing usage of nanosilver-containing products, people are more likely to be exposed to AgNPs. Due to the small size, AgNPs are capable

Correspondence: Ying Liu; Liming Xie
National Center for Nanoscience and Technology, No.11. Beiyitiao Zhongguancun, Haidian District, Beijing 100190, People's Republic of China
Tel +86 108 254 5665
Fax +86 106 265 6765
Email liuy1@nanoctr.cn; xielm@nanoctr.cn

submit your manuscript | www.dovepress.com
DovePress
http://doi.org/10.2147/IJN.S201107

© 2019 Wu et al. This work is published and licensed by Dove Medical Press Limited. The full terms of this license are available at https://www.dovepress.com/terms.php and incorporate the Creative Commons Attribution – Non Commercial (unported, v3.0) License (http://creativecommons.org/licenses/by-nc/3.0/). By accessing the work you hereby accept the Terms. Non-commercial uses of the work are permitted without any further permission from Dove Medical Press Limited, provided the work is properly attributed. For permission for commercial use of this work, please see paragraphs 4.2 and 5 of our Terms (https://www.dovepress.com/terms.php).

of entering the human body by inhalation, skin penetration, ingestion, and/or injection. Liver, lung, spleen, and kidney are the main target organs for nanosilver accumulation in vivo.[12,13] As a result, the particles might be taken up into cells, leading to potential hazards by interaction with intracellular biological macromolecules. Uptake pathways and cellular distribution of AgNPs directly correlated with various cytotoxic effects. So, it is imperative to explore the pathways of cellular uptake and the intracellular behaviors of exogenous AgNPs, which can help us better understand their biological effects and optimize their biomedical applications.

Generally, nanoparticles may enter cells by mechanisms of phagocytosis, micropinocytosis, endocytosis, direct diffusion, or adhesive interactions.[14] The ways in which nanoparticles are internalized by cells are determined by their physical and chemical properties, such as size, shape, surface charge, and composition.[15–18] In recent years, several previous studies hinted that, in the process of cellular uptake of liposomes, quantum dots, gold and silica nanoparticles, the size was found to be an essential factor.[19–21] It is likely that smaller NPs are imported into cells via endocytosis or diffusion, and larger NPs are via phagocytosis in the previous research.[22,23] In terms of AgNPs, most uptake studies focused on the uptake efficiency and toxicity, but the exact mechanisms of cellular uptake for AgNPs in mammalian cells have not been well characterized.

The purpose of our present study is to investigate the size effects of AgNPs on the internalization pathways by cells and their intracellular localizations. Tumor cell lines are often used as models for studying nanoparticle-cell interactions. Here, the mouse melanoma cell line (B16), a kind of non-phagocytic epithelioid cells, was chosen as an experimental model suitable for our uptake research. We mainly analyzed the uptake behaviors of AgNPs in different sizes by transmission electron microscopy (TEM) and inductively coupled plasma-mass spectrometry (ICP-MS) in B16 cells. Our results show that the cellular uptake of AgNPs was size-dependent, and the maximum uptake efficiency occurred at the particle size of 100 nm. The results after the treatment of specific endocytic inhibitors revealed that more than one internalization pathway might be involved in the internalization process of AgNPs.

Materials and methods

Materials

RPMI 1640, streptomycin/penicillin, and PBS were purchased from Cellgro (VA, US). Fetal bovine serum (FBS) was purchased from Hyclone (UT, USA). Glutamax was purchased from Gibco (CA, US). Citrate-coated AgNPs (5 nm, 20 nm, 50 nm, 100 nm) were from Nanocomposix (CA, US). CellTiter 96® Aqueous One Solution Reagent was from Promega (WI, USA). Glutaraldehyde was bought from Sinopharm chemical reagent Co., Ltd (Shanghai, China). Dodecenyl succinic anhydride (DDSA), methyl nadic anhydride (MNA), 2,4,6 Tri (dimethylaminomethyl) phenol (DMP-30), Epon-812, and OsO_4 were from Sigma-Aldrich (China). All chemicals used for digestion and ICP-MS were of metal-oxide-semiconductor (MOS) grade. Nitric acid (HNO_3) was purchased from Beijing Institute of Chemical Reagents (Beijing, China).

Cell cultures

B16 mouse melanoma cell line (B16) from American Type Culture Collection (ATCC) was kindly given by Dr. Guangjun Nie from NCNST and cultured in RPMI 1640 complete medium with 10% fetal bovine serum (FBS), streptomycin/penicillin (100 U/mL), and Glutamax (2 mM) at 37°C in a humidified atmosphere of 5% CO_2 incubator.

Characterization of AgNPs

Six microliters of AgNPs dispersed in Milli-Q water was dropped on TEM grid and dried for transmission electron microscopic (TEM) imaging. The TEM imaging was conducted on Tecnai G2 F20 U-TWIN (FEI, USA) at an acceleration voltage of 200 kV. The sizes and zeta potentials of AgNPs at the concentration of 10 μg/mL were measured in different media by dynamic light scattering (DLS) (Zetasizer Nano ZS, Malvern, UK) at 25°C. For each sample, DLS was repeated at least three measurements, and each measurement was at least 12 individual runs. The SpectraMax® i3 microplate reader (Molecular Devices, Sunnyvale, CA, USA) was used for measuring the UV/visible absorption spectrum of AgNPs.

Cytotoxicity of AgNPs (MTS assay)

The cytotoxicity of AgNPs in B16 cells was detected by the Aqueous One Solution Reagent (Promega). B16 cells were trypsinized and suspended in complete medium. A 200 μL cell suspension (5×10^4 cells/mL) per well was added in a flat-bottom 96-well plate and cultured overnight at 37°C in a 5% CO_2 humidified incubator. Then, cells were incubated with different concentrations (5–100 μg/mL) of AgNPs for 24 hours. After cell wash with PBS, cell viability was determined by MTS (3-(4,

5-dimethylthiazol-2-yl)-5- (3-carboxymethoxyphenyl)-2-(4-sulfophenyl)-2H- tetrazolium, inner salt) assay according to manufacturer's instructions; 20 μL of MTS reagent was added directly into each well. After 2 hours incubation at 37°C in a 5% CO_2 humidified incubator, the absorbance was determined at 490 nm by the microplate reader.

The preparation of cell samples prior to ICP-MS measurement

Cells were collected and pre-digested with 1 mL nitric acid (HNO_3) overnight. Then digested products were transferred to PFA (perfluoroalkyl alkanes) digestion vessels with another 9 mL of nitric acid, followed by a microwave heating program for digestion (120°C for 2 minutes, 160°C for 5 minutes, and 195°C for 50 minutes). After cooling down, the vessels were heated to about 150°C in a heating block (BHW-09C, BOTONYC, Shanghai, China) and diluted with 1% (v/v) HNO_3 to a final acid concentration of ~3% before ICP-MS measurement. Each sample was prepared in triplicate.

The uptake of AgNPs by B16 cells by ICP-MS measurement

The total silver contents in samples were determined by ICP-MS (NexION 300X, Perkin Elmer, USA). In (25 ppb) was used as the internal standard correction. The main working conditions of ICP-MS measurement were as follows: the radio frequency (RF) power was 1,600 W; and argon gas flow rates for the plasma, auxiliary, and nebulizer flow were 18 L/min, 1.2 L/min, and 0.98 L/min, respectively.

Intracellular distribution of AgNPs in B16 cells by TEM

B16 cells cultured in 6-well plates were treated with different-sized AgNPs at 15 μg/mL in the FBS-free RPMI 1640 medium. After being cultured for 12 hours or 24 hours, cells were washed by PBS three times, digested, and centrifuged. The cell pellets were quickly fixed within 2.5% (v/v) glutaraldehyde in 0.1 M sodium phosphate buffer (pH 7.4) overnight. Then, cells were washed adequately and fixed in 1% OsO_4 (w/v) for 1.5 hours subsequently. After washing, cell pellets were dehydrated in a graded series of acetone, then transferred to a graded series of embedding medium containing dodecenyl succinic anhydride (DDSA), methyl nadic anhydride (MNA), 2,4,6 Tri (dimethylaminomethyl) phenol (DMP-30), and Epon-812, and finally embedded in pure Epon-812. The sections from embedded cell blocks were collected on a copper grid for observation by TEM. To avoid the dye pollution, the sections were not stained with uranyl acetate and lead citrate.

The uptake of AgNPs after inhibitor treatments

B16 cells were seeded in 6-well plates under cell culture conditions. After 24 hours growing, cells were treated with 25 μM chlorpromazine hydrochloride (CPZ, Sigma Aldrich), 100 μM 5-(N-ethyl-N-isopropyl) amiloride (EIPA) (Toronto research chemicals, ON, Canada) for 30 minutes, and 5 mM Mβ-CD (methyl-β-cyclodextrin) (Sigma Aldrich) for 1 hour at 37°C. CPZ can specifically inhibit the clathrin-mediated endocytosis. Mβ-CD is a specific caveolin-mediated endocytosis inhibitor. EIPA is an inhibitor of macropinocytosis. Then, AgNPs were added into wells and incubated for another 2 hours. Subsequently, cells were washed with PBS twice, and collected for ICP-MS analysis.

Statistical analysis

Data were presented as mean±SD from at least three independent experiments. Statistical differences between groups were compared by one-way analysis of variance (ANOVA). $P<0.05$ was considered as a significant difference.

Results

Characterization study of AgNPs

The physicochemical properties of four CIT-coated AgNPs (5 nm, 20 nm, 50 nm, 100 nm) used in our study were characterized by TEM, DLS, and UV-Vis spectroscopy. TEM images confirmed the sphere morphology and the size distributions were 3.2±0.5 nm (Figure 1A), 20.7±2.5 nm (Figure 1B), 54.7±7.7 nm (Figure 1C), and 93.6±9.6 nm (Figure 1D), respectively. The hydrodynamic sizes (d_H) and zeta potentials (ζ) of all AgNPs in water as well as in culture media are summarized in Table 1. In water solution, there was no aggregation for CIT-coated AgNPs with diameters of 20, 50, and 100 nm. But there was slight aggregation for 5 nm AgNPs as the hydrodynamic diameter was 11.8±0.9 nm measured from DLS. In culture media without serum, there was much more aggregation for all AgNPs (d_H>600 nm), indicating the culture media can facilitate AgNPs aggregation.[24,25] Moreover, zeta potentials in culture medium without serum were less

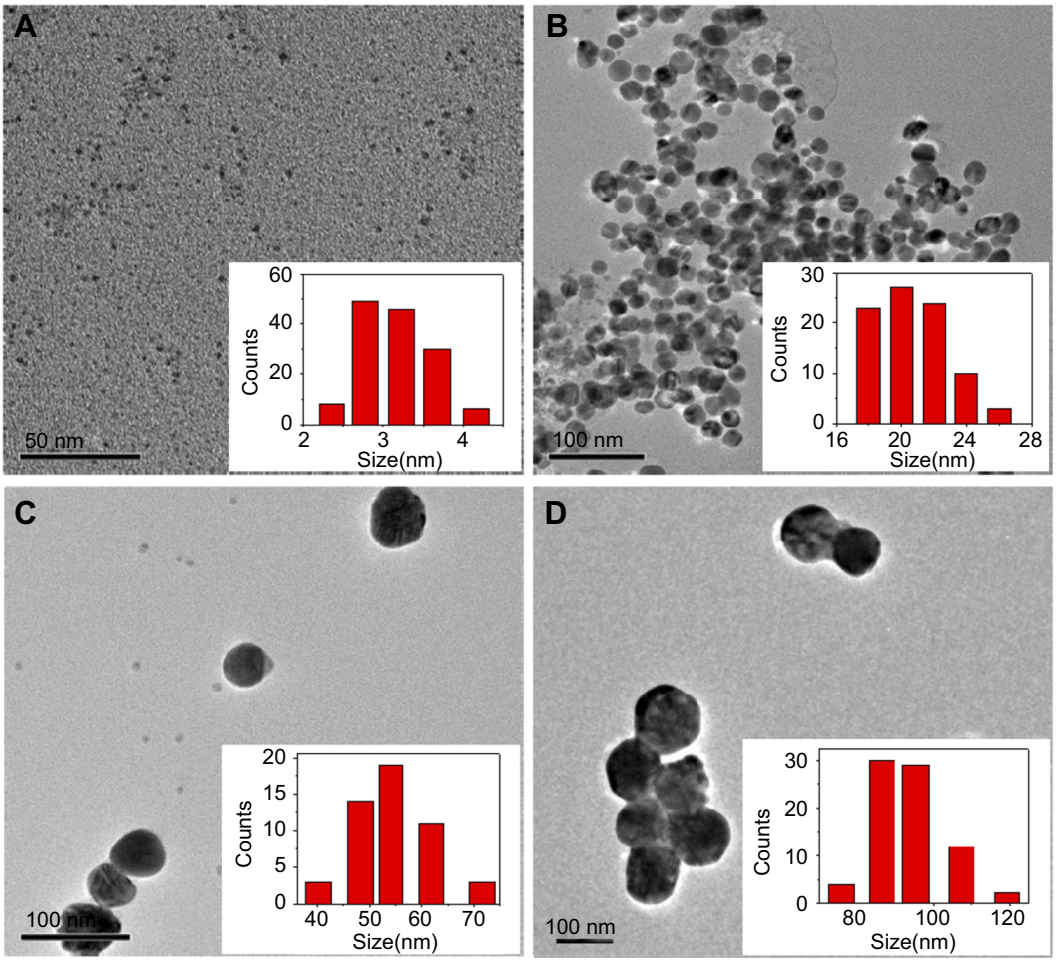

Figure 1 The morphology images and size distributions by TEM for 5 nm (**A**), 20 nm (**B**), 50 nm (**C**), and 100 nm (**D**) AgNPs.
Abbreviations: AgNPs, silver nanoparticles; TEM, transmission electron microscopy.

Table 1 Physicochemical properties of AgNPs by TEM and DLS

Characterization	AgNP-5	AgNP-20	AgNP-50	AgNP-100
TEM size (nm)	3.2±0.5	20.7±2.5	54.3±7.7	93.6±9.6
Morphology	Sphere	Sphere	Sphere	Sphere
λ_{max}/nm (water)	400	395	420	505
d_H/nm (water)	11.8±0.9	27.4±0.4	55.2±0.3	103.6±0.8
ζ/mV (water)	−24.7±0.8	−30.1±1.1	−39.6±0.3	−42.8±0.2
d_H/nm (medium)	614.2±34.7	677.0±16.5	672.1±16.5	722.7±27.8
ζ/mV (medium)	−12.2±1.3	−11.2±1.3	−10.9±0.3	−10.0±0.5

Abbreviations: AgNP, silver nanoparticles; DLS, dynamic light scattering; TEM, transmission electron microscopy; d_H, hydration diameter; ζ, zeta potential.

negative than those in water. UV-Vis absorption spectra of AgNPs are shown in Figure S1.

The size-dependent uptake efficiency of AgNPs by B16 cells

First, the cytotoxicity of AgNPs to B16 cells was evaluated by MTS assay to determine the optimum dose in the following experiments. As shown in Figure S2, only 5 nm AgNPs significantly inhibited the viability of B16 cells up to about 60% at high concentrations of 75 and 100 μg/mL, which is consistent with other reports.[26] According to these results, a concentration of 15 μg/mL of AgNPs was used in the following experiments.

To calculate the uptake efficiency of AgNPs, the amount of silver (Ag) internalized by B16 cells at 12 hours or 24 hours

after co-culture with AgNPs was quantitatively measured by ICP-MS. The average recovery of standard silver ion (Ag^+) solution by this method was determined to ensure the accuracy and precision of subsequent experiments. Figure S3 indicatesthat the detection limit of Ag in microwave-digest method was 0.003 μg, and good recovery efficiency was achieved in the range of 0.005–100 μg. After method validation, the Ag content inside B16 cells was measured. As shown in Figure 2, the uptake efficiencies after 12 hours exposure were 40.3 ±7.6%, 22.0±1.5%, 52.3±4.7%, and 76.2±8.0% for 5 nm, 20 nm, 50 nm, and 100 nm AgNPs, respectively. For 24 hours exposure, the uptake efficiency of AgNPs increased slightly to 58.5±8.5%, 34.2±8.3%, and 57.9±2.5% for 5 nm, 20 nm, and 50 nm AgNPs, respectively. However, for 100 nm AgNPs, the uptake slightly decreased to 66.1±9.7% (Figure 2). Interestingly, at both 12 hour and 24 hour uptake experiments, 20 nm and 100 nm AgNPs showed the lowest and highest uptake efficiency in B16 cells, respectively.

The interaction between AgNPs and plasma membrane

TEM imaging was used to evaluate the locations of AgNPs at different time points during the uptake process in B16 cells. After 0.5 hours of co-culture, 5 nm AgNPs had already entered cells through the cell membrane. The 5 nm AgNPs were uniformly distributed in the cytoplasm and nucleus, while most of the AgNPs with bigger sizes (20 nm, 50 nm, 100 nm) were still located outside the cells (Figure 3). Interestingly, we captured some images indicating the interaction between AgNPs and cell membrane. The 5 nm AgNPs were loaded in some nano-sized vesicle-like structures outside the cell membrane (Figure 3A). A trend of cell membrane invagination can be observed for 20 nm, 50 nm, and 100 nm AgNPs (Figures 3B–D).

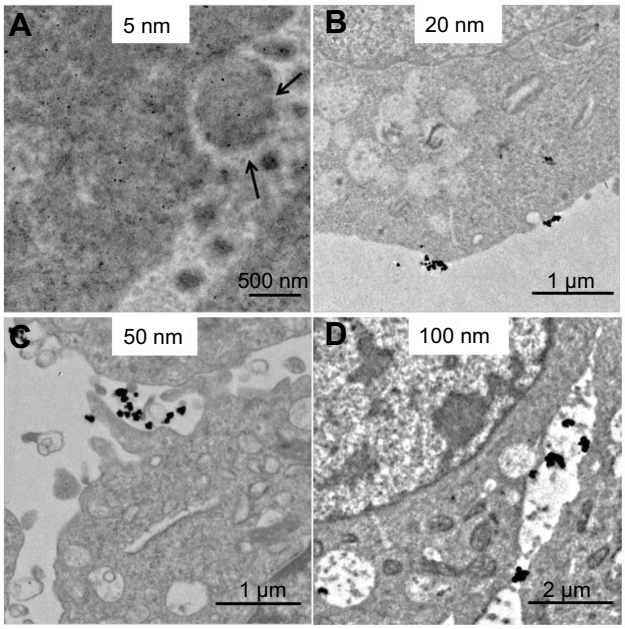

Figure 3 Interaction of AgNPs with plasma membrane after 0.5 hours exposure by TEM analysis. (**A**–**D**) The representative TEM images of 5 nm, 20 nm, 50 nm, and 100 nm AgNPs. Black arrows, vesicle-like structures outside the cell membrane.
Abbreviations: AgNPs, silver nanoparticles; TEM, transmission electron microscopy.

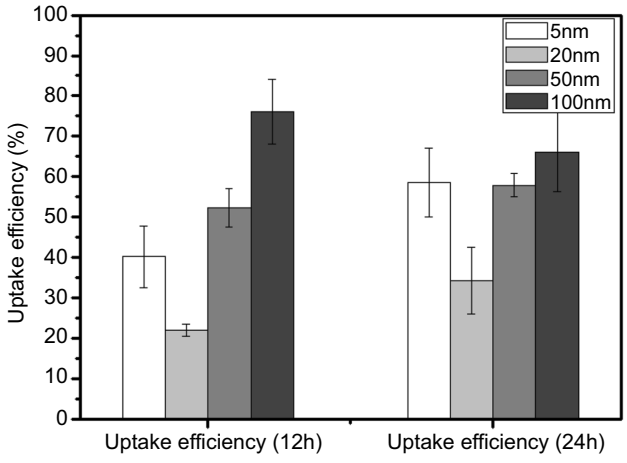

Figure 2 Uptake efficiency of AgNPs in B16 cells. After the incubation of 12 hours or 24 hours, AgNPs-treated cells were collected for ICP-MS analysis to determine the intracellular content of Ag. The uptake efficiency was calculated by the intracellular content divided by total Ag input (Mean±SD, n=6 for each group).
Abbreviations: AgNPs, silver nanoparticles; Ag, silver; ICP-MS, inductively coupled plasma mass spectrometry.

Time-dependent intracellular localization of AgNPs in B16 cells

After 0.5 hours co-culture, a few of the 20 nm AgNPs can also be observed in the nucleus, besides 5 nm AgNPs (Figure 4A). However, there was still no 50 nm or 100 nm AgNPs in the nucleus (Figure 4A). After 2 hours of co-culture, AgNPs in all four sizes were observed to be taken up by B16 cells (Figure 4B). The 5 nm AgNPs were still uniformly dispersed in the cytoplasm and nucleus. The 20 nm, 50 nm, and 100 nm AgNPs were mainly localized within membrane-bound structures as endocytic vesicles, especially in early endosomes and lysosomes. Usually, these special structures can be identified as they were surrounded by a membrane and had a distinct electron contrast (Figure 4B). Additionally, at this time point, 50 nm AgNPs was able to enter the nucleus, but not for 100 nm particles.

After 12 hours of exposure to AgNPs, different from short-time points, some larger membrane vesicles inside cells were observed with loaded bigger-sized AgNPs (20

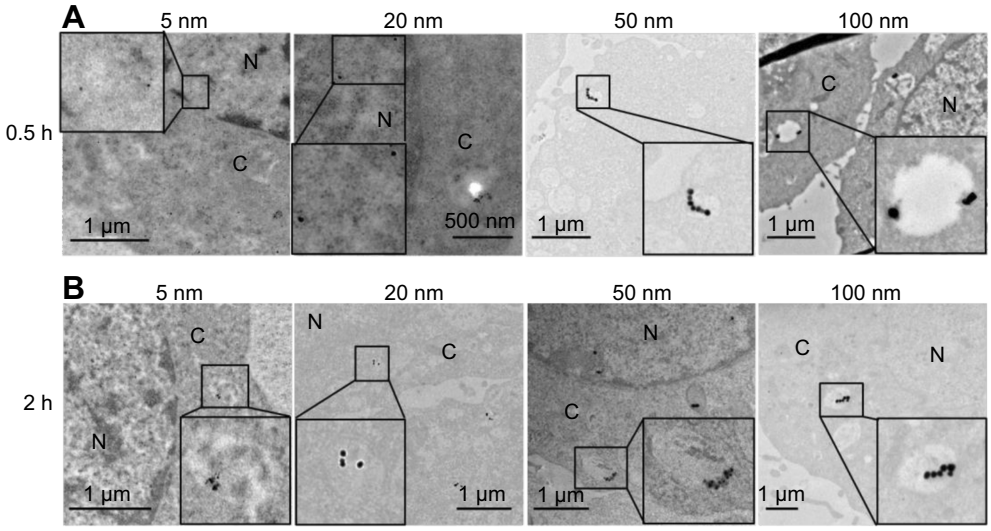

Figure 4 The cellular distribution of AgNPs after 0.5 hours (**A**) and 2 hours (**B**) exposure in B16 cells. From left to right, the four panels display the representative TEM images of 5 nm, 20 nm, 50 nm, and 100 nm AgNPs, respectively.
Abbreviations: AgNPs, silver nanoparticles; TEM, transmission electron microscopy; N, nucleus; C, cytoplasm.

nm, 50 nm, 100 nm) (Figures 5B–D). However, we cannot find any 5 nm AgNPs located in such large membrane vesicles within cells (Figure 5A). In addition, almost all internalized AgNPs showed less tendency of aggregation compared with those outside the cell membrane. Moreover, none of the 100 nm AgNPs was observed in the nucleus, even after 12 hours.

Possible uptake pathways for different-sized AgNPs by B16 cells

To further investigate potential endocytic mechanisms for different-sized AgNPs, some selective inhibitors were used to check the effects on the uptake efficiency of AgNPs. First, none of these inhibitors affected the cell viability (data not shown). After pre-incubation with the individual inhibitor, cells were co-cultured with AgNPs for another 2 hours. As shown in Figure 6, the uptake of all four-sized AgNPs decreased significantly after the pre-treatment with CPZ, which can specifically inhibit the clathrin-mediated endocytosis. In the presence of a specific caveolin-mediated endocytosis inhibitor (Mβ-CD), the internalization efficiencies of AgNPs with 5 nm size (Figure 6A), 20 nm size (Figure 6B), and 50 nm size (Figure 6C) were markedly reduced. Specifically, the internalization of AgNPs with both 5 nm and 50 nm exhibited an inhibition rate of approximately 50% in B16 cells. The uptake of larger sizes of AgNPs (50 nm and 100 nm) was inhibited by EIPA (an inhibitor of macropinocytosis) by more than 20% compared with the control (Figures 6C and D). Remarkably, only B16 cells exposed to 50 nm AgNPs maintained low uptake efficiency by pre-treatment with all three different inhibitors.

Discussion

The uptake of nanoparticles can be affected by various factors, such as physicochemical properties of nanoparticles, protein adsorption, and cell types.[20,27–29] The purpose of the present study is to investigate the size effects on the specific pathways of AgNPs entry and processing by B16 cells, a non-phagocytic cell line. To avoid the impacts of the protein adsorption, this study was conducted in serum free system. The only variable parameter of AgNPs is size, which was confirmed by the characterization results (Figure 1, Table 1). First, we checked the size-dependence of cellular uptake for AgNPs by ICP-MS. There have already been some publications to investigate the uptake efficiency of nanoparticles. In some culture cell lines, a size-dependent uptake has been observed for AuNPs,[20,30,31] mesoporous silica,[19] polystyrene,[32] iron oxide nanoparticles,[33] and AgNPs.[34] They all have a maximum efficiency of cellular uptake at some particle size in the range of 30−50 nm. Middle sized AgNPs (50 nm) also exhibited the highest level of absorption and uptake in red blood cells (RBCs).[35] These results suggested that there might be an optimal particle size for active uptake in a relatively short incubation time (less than 4 hours).[35] In this study, we obtained the different uptake tendency of AgNPs in B16 cells. Our ICP-MS results showed that 20 nm AgNPs had the lowest

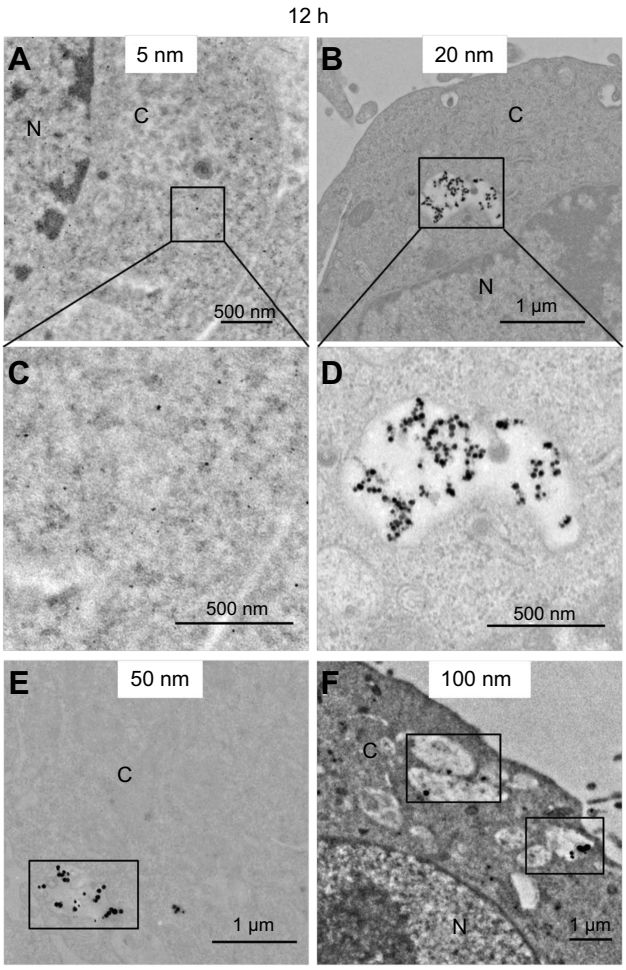

Figure 5 AgNPs uptake by B16 cells after 12 hours incubation. (**A**, **B**, **E**, **F**) The representative TEM images of 5 nm, 20 nm, 50 nm, and 100 nm AgNPs. (**C**, **D**) The amplified images of **A** and **B**, respectively.
Abbreviations: AgNPs, silver nanoparticles; TEM, transmission electron microscopy; N, nucleus; C, cytoplasm.

efficiency after both 12 hours and 24 hours exposure, while AgNPs at the sizes of 50 and 100 nm had higher uptake efficiencies. However, our data were not totally incompatible with the previous results. Here, the longer incubation time (12 hours/24 hours) was chosen in this experiment, since we intend to explore the association between the uptake and toxicity of AgNPs. Thus, although we mainly focused on the endocytosis of AgNPs in this period, the exocytosis should also be considered in this process. In fact, the uptake efficiency calculated here was a net value subtracted by the exocytic particles. Our unpublished data have already suggested that AgNPs at different sizes displayed different exocytosis efficiency at 12 hours or 24 hours (unpublished data). Therefore, our results implied that, for long interaction duration (>12 hours), the internalization process of larger AgNPs (50 nm and 100 nm) in B16 cells was much more effective. In combination with TEM results, the smaller AgNPs (20 nm) may enter B16 cells less effectively, since these particles go into and out of cells more easily.

As we know, eukaryotic cells are multi-compartmented. The trafficking of exogenous materials in cells mainly depends on the exchange of membrane enclosed vesicles.[36] When exposed to nanoparticles, cells got the signal and internalized the particles by membrane invagination, and then the invagination pinched off to form new intracellular vesicles.[37,38] A similar phenomenon was observed in our study, as shown in Figures 3 and 4. Furthermore, bio-TEM analysis showed that AgNPs were taken up and mainly localized within membrane-bound structures, similar to Gia et al[34] and Milić et al.[39] The 20 nm, 50 nm, and 100 nm AgNPs can be observed in early endosomes originatingfrom membrane invagination (Figure 4), which then fused into late endosomes by multiple units (Figure 5). In addition, it has been reported by Krpetic et al[40] that TAT-modified AuNPs can enter HeLa cells as single particles. Thus, we supposed that some single AgNPs may also directly cross the membrane to reach the cytoplasm, possibly by direct membrane translocation. The exact mechanisms mediating the penetration of AgNPs with different sizes through the membrane still remain to be elucidated. Moreover, the existence of single nanoparticle in the cytoplasm may have resulted from endosomal escape. Hence, we assumed that the endosomal escape of AgNPs may be due to the damage of charge balance and/or the membrane ruptures caused by silver ions released from AgNPs.[41] Meanwhile, our results about the AgNPs localizations in membrane-bound structures also gave us some hints about multiple endocytic mechanisms of AgNPs in B16 cells. We suspected that direct membrane translocation and clathrin/caveolin mediated endocytosis may be responsible for the intravesicular translocation of AgNPs.

As a process of active transport, endocytosis is a fundamental process of internalizing macromolecules, bacteria, and viruses by cells. It is also a major pathway of cellular uptake for nanoparticles.[36] It has been reported that clathrin-mediated and macropinocytic endocytosis are involved, but there might still be other uptake pathways for 50±20 nm PVP-coated AgNPs in hMSC.[42] Another study by Gliga et al[34] showed that the overall uptake of 10 nm and 70 nm PVP-coated AgNPs in human lung cells was a combination of active mechanisms including clathrin, caveolin/lipid raft, macropinocytosis, and phagocytosis. In the present study, we utilized some specific endocytic inhibitors to explore the distinct

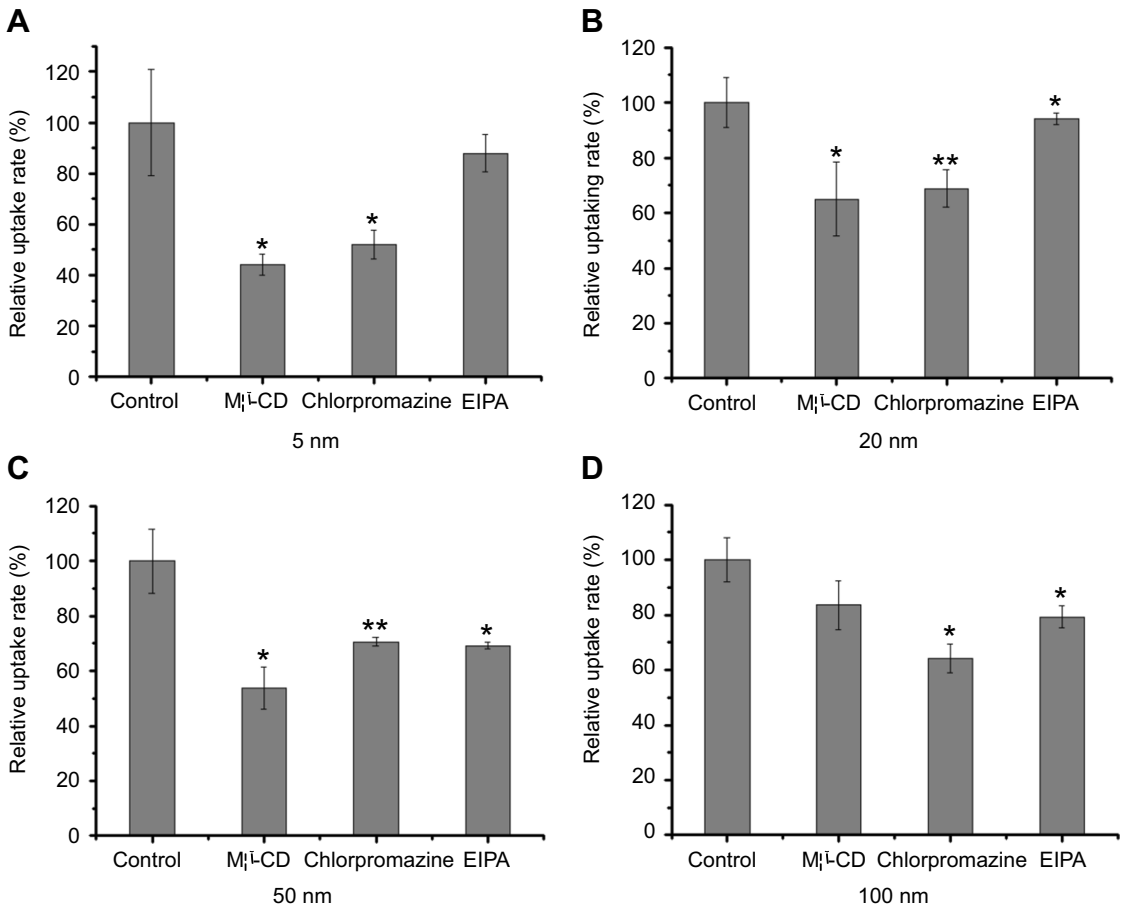

Figure 6 The relative uptake rate of different-sized AgNPs after inhibitor treatments in B16 cells. Cells were separately pretreated with Mβ-CD, CPZ, and EIPA before the addition of AgNPs (Mean±SD, n=4. *P<0.05, **P<0.01, significantly different from the control group). (**A-D**) The representative result for 5 nm, 20 nm, 50 nm , 100 nm AgNPs, respectively.

Abbreviations: AgNPs, silver nanoparticles; Mβ-CD, methyl-β-cyclodextrin; CPZ, chlorpromazine hydrochloride, EIPA, 5-(N-ethyl-N-isopropyl) amiloride.

pathways of AgNPs internalization. Mβ-CD, CPZ, and EIPA as the pharmaceutical inhibitors were used to specifically inhibit caveolae-mediated, clathrin-mediated, and macropinocytic endocytosis, respectively. The result of endocytosis inhibition assay implied that macropinocytosis might only be involved in the internalization of larger-sized AgNPs (50 nm and 100 nm), as shown in Figure 6, since the macropinocytic inhibitor EIPA just brought about minor inhibition for the cellular uptake of smaller AgNPs (5 nm and 20 nm).

In addition, the previous results showed that lipoplexes with a diameter of 200 nm or less were primarily internalized through the pathway of clathrin-mediated endocytosis.[43] Similarly in the present study, it was noted that the significant uptake suppression after the treatment of chlorpromazine illustrated that clathrin-mediated endocytosis contributed to the internalization of all four-sized AgNPs. Therefore, we deduced that clathrin-mediated endocytosis might be a general pathway of active uptake for citrate-coated AgNPs in B16 cells. This further suggests that clathrin-mediated endocytosis is a conserved mechanism exploited by eukaryotic cells to internalize foreign materials. In addition, Mβ-CD markedly reduced the efficiency of cellular uptake for 5 nm, 20 nm, and 50 nm AgNPs, indicating that the caveolae-mediated pathway mainly participated inendocytosis of AgNPs at a size of less than 50 nm.

Interestingly, we also noticed that different sized AgNPs displayed different profiles after the treatment of some specific endocytic inhibitors, and the inhibitory extent for a single inhibitor was also distinct. Accordingly, it could be supposed that AgNPs at a certain size can take a combination of various pathways to enter cells, but there must be only one major pathway in this process. In the light of our data, very small AgNPs (~5 nm) may mainly accomplish the endocytosis by the caveolae-mediated pathway with a supply of clathrin-mediated pathway. While the most important endocytic pathways for ~20 nm AgNPs might be the clathrin-

mediated endocytosis, ~50 nm AgNPs would take three endocytic pathways to implement their internalization, among which the caveolae-mediated endocytosis may occur more easily. The clathrin-mediated pathway, along with the macropinocytosis, also played a primary role in the uptake of quite large AgNPs (~100 nm). In addition, AgNPs aggregation status might be another possible reason for adopting different uptake pathways. We also speculated about a potential compensatory mechanism during the treatment of a single inhibitor. Although one single endocytic inhibitor can specifically impact one endocytic pathway, there might be other alternative pathways which compensated for the inhibitory effects. Thereby, the influence produced by one inhibitor was considered as an integrated result. Naturally, the internalization pathway of AgNPs must also be influenced by other factors, such as surface-coating and cell types. However, the size effects should be much more profound than any other factors for the uptake mechanisms. Hereby, our findings indicated that AgNPs should be carefully designed for different applications in biomedical fields, particularly in respect of their sizes.

The location of nanoparticles in the nucleus greatly influences cell functions, because it is likely that these nanoparticles cannot be eliminated from cells according to previous studies.[44] There are some nuclear pore complexes (NPCs) on the nuclear membrane in living cells, the diameter of which is ~20–50 nm depending on cell types.[45,46] So, small nanoparticles can pass NPCs on the nuclear membrane so as to enter the nucleus. Several studies have shown that nanoparticles with a diameter smaller than 40 nm can enter the nucleus.[47,48] The nuclear location of AgNPs has also been previously reported.[49–51] Hackenberg et al[52] confirmed that AgNPs (<50 nm) could enter the nucleus of human mesenchymal stem cells (hMSC) which were in coincidence with our ultrastructural results about the nuclear localization of 5 nm, 20 nm, and 50 nm AgNPs after 2 hours incubation (Figure 4). Furthermore, our results also showed that almost no 100 nm AgNPs were observed in the nucleus of B16 cells, even after 12 hours incubation, which gave a reasonable explanation about lower cytotoxicity of 100 nm AgNPs than another three sized AgNPs (Figure S2).

Conclusion

Taken together, ICP-MS data has clearly shown that the uptake efficacy of AgNPs is correlated with particle sizes. The 20 nm and 100 nm AgNPs had the lowest and highest uptake efficiency, respectively. This revealed that 20 nm can go into and go out of cells more easily. We have directly observed the internalized AgNPs mainly existed within membrane-bound structures, such as intracellular vesicles and late endosomes. The entry of AgNPs into the nucleus has been confirmed to be size- and time-dependent. Then, according to TEM results, we further figured out the dependency of the endocytic pathway on size by inhibitory assay. Based on the results after adding some specific endocytic inhibitors, we have discovered that AgNPs at any size may involve more than one endocytic pathway. Although there are multiple uptake pathways for all four-sized particles, each size of AgNPs has been identified to enter cells through a major pathway. Moreover, it could be proposed that the clathrin-mediated endocytosis could be regarded as the most common pathway for AgNPs in mammalian cells. Our results and conclusions are quite essential to understand the exact interaction mechanism between AgNPs and cells. Our study about the endocytic pathways of AgNPs would provide very important information for the development of drug delivery and for the risk assessment of AgNPs in practical applications.

Acknowledgments

This study is financially supported by the National Natural Science Foundation of China (grant number 31600814) and "Strategic Priority Research Program" of Chinese Academy of Sciences (grant number XDA09040300).

Disclosure

The authors report no conflicts of interest in this work.

References

1. Zhang L, Lu Z, Bai Y, et al. PEGylated denatured bovine serum albumin modified water-soluble inorganic nanocrystals as multifunctional drug delivery platforms. *J Mater Chem B*. 2013;1:1289–1295. doi:10.1039/c2tb00380e
2. Biju V. Chemical modifications and bioconjugate reactions of nanomaterials for sensing, imaging, drug delivery and therapy. *Chem Soc Rev*. 2014;43(3):744–764. doi:10.1039/c3cs60273g
3. Vasantharaj S, Sathiyavimal S, Senthilkumar P, LewisOscar F, Pugazhendhi A. Biosynthesis of iron oxide nanoparticles using leaf extract of Ruellia tuberosa: antimicrobial properties and their applications in photocatalytic degradation. *J Photochem Photobiol B*. 2019;192:74–82.
4. Shanmuganathan R, MubarakAli D, Prabakar D, et al. An enhancement of antimicrobial efficacy of biogenic and ceftriaxone-conjugated silver nanoparticles: green approach. *Environ Sci Pollut Res*. 2018;25(11):10362–10370.
5. Pugazhendhi A, Prabakar D, Jacob JM, Karuppusamy I, Saratale RG. Synthesis and characterization of silver nanoparticles using Gelidium amansii and its antimicrobial property against various pathogenic bacteria. *Microb Pathog*. 2018;114:41–45.
6. Saravanan M, Arokiyaraj S, Lakshmi T, Pugazhendhi A. Synthesis of silver nanoparticles from Phenerochaete chrysosporium (MTCC-787) and their antibacterial activity against human pathogenic bacteria. *Microb Pathog*. 2018;117:68–72.

7. Saravanan M, Barik SK, MubarakAli D, Prakash P, Pugazhendhi A. Synthesis of silver nanoparticles from Bacillus brevis (NCIM 2533) and their antibacterial activity against pathogenic bacteria. *Microb Pathog*. 2018;116:221–226.
8. Oves M, Aslam M, Rauf MA, et al. Antimicrobial and anticancer activities of silver nanoparticles synthesized from the root hair extract of Phoenix dactylifera. *Mater Sci Eng C Mater Biol Appl*. 2018;89:429–443.
9. Vasantharaj S, Sathiyavimal S, Saravanan M, et al. Synthesis of ecofriendly copper oxide nanoparticles for fabrication over textile fabrics: characterization of antibacterial activity and dye degradation potential. *J Photochem Photobiol B*. 2019;191:143–149.
10. Roe D, Karandikar B, Bonn-Savage N, Gibbins B, Roullet JB. Antimicrobial surface functionalization of plastic catheters by silver nanoparticles. *J Antimicrob Chemother*. 2008;61(4):869–876. doi:10.1093/jac/dkn034
11. Wijnhoven SWP, Peijnenburg WJGW, Herberts CA, et al. Nano-silver–a review of available data and knowledge gaps in human and environmental risk assessment. *Nanotoxicology*. 2009;3:109–138. doi:10.1080/17435390902725914
12. Wu M, Chen L, Li R, et al. Bio-distribution and bio-availability of silver and gold in rat tissues with silver/gold nanorod administration. *RSC Adv*. 2018;8:12260–12268. doi:10.1039/C8RA00044A
13. Walker M, Parsons D. The biological fate of silver ions following the use of silver-containing wound care products - a review. *Int Wound J*. 2014;11(5):496–504. doi:10.1111/j.1742-481X.2012.01115.x
14. De Lima R, Seabra AB, Durán N. Silver nanoparticles: a brief review of cytotoxicity and genotoxicity of chemically and biogenically synthesized nanoparticles. *J Appl Toxicol*. 2012;32:867–869. doi:10.1002/jat.2780
15. Chung TH, Wu SH, Yao M. The effect of surface charge on the uptake and biological function of mesoporous silica nanoparticles in 3T3-L1 cells and human mesenchymal stem cells. *Biomaterials*. 2007;28:2959–2966. doi:10.1016/j.biomaterials.2007.03.006
16. Rejman J, Oberle V, Zuhorn IS, Hoekstra D. Size-dependent internalization of particles via the pathways of clathrin- and caveolae-mediated endocytosis. *Biochem J*. 2004;377(Pt 1):159–169. doi:10.1042/BJ20031253
17. Chithrani BD, Chan WC. Elucidating the mechanism of cellular uptake and removal of protein-coated gold nanoparticles of different sizes and shapes. *Nano Lett*. 2007;7(6):1542–1550. doi:10.1021/nl070363y
18. Gratton SE, Ropp PA, Pohlhaus PD, et al. The effect of particle design on cellular internalization pathways. *Proc Natl Acad Sci U S A*. 2008;105(33):11613–11618. doi:10.1073/pnas.0801763105
19. Lu F, Wu SH, Hung Y, Mou CY. Size effect on cell uptake in well-suspended, uniform mesoporous silica nanoparticles. *Small*. 2009;5(12):1408–1413. doi:10.1002/smll.200900005
20. Chithrani BD, Ghazani AA, Chan WC. Determining the size and shape dependence of gold nanoparticle uptake into mammalian cells. *Nano Lett*. 2006;6(4):662–668. doi:10.1021/nl052396o
21. Peruzynska M, Cendrowski K, Barylak M, et al. Study on size effect of the silica nanospheres with solid core and mesoporous shell on cellular uptake. *Biomed Mater*. 2015;10(6):065012.
22. Conner SD, Schmid SL. Regulated portals of entry into the cell. *Nature*. 2003;422(6927):37–44.
23. Marchesano V, Hernandez Y, Salvenmoser W, et al. Imaging inward and outward trafficking of gold nanoparticles in whole animals. *ACS Nano*. 2013;7(3):2431–2442.
24. Wang X, Ji Z, Chang CH, et al. Use of coated silver nanoparticles to understand the relationship of particle dissolution and bioavailability to cell and lung toxicological potential. *Small*. 2014;10(2):385–398.
25. Lee YH, Cheng FY, Chiu HW, et al. Cytotoxicity, oxidative stress, apoptosis and the autophagic effects of silver nanoparticles in mouse embryonic fibroblasts. *Biomaterials*. 2014;35(16):4706–4715.
26. Sur I, Cam D, Kahraman M, Baysal A, Culha M. Interaction of multi-functional silver nanoparticles with living cells. *Nanotechnology*. 2010;21(17):175104.
27. Qiu Y, Liu Y, Wang L, et al. Surface chemistry and aspect ratio mediated cellular uptake of Au nanorods. *Biomaterials*. 2010;31(30):7606–7619.
28. Tedja R, Lim M, Amal R, Marquis C. Effects of serum adsorption on cellular uptake profile and consequent impact of titanium dioxide nanoparticles on human lung cell lines. *ACS Nano*. 2012;6(5):4083–4093.
29. Coulter JA, Jain S, Butterworth KT, et al. Cell type-dependent uptake, localization, and cytotoxicity of 1.9 nm gold nanoparticles. *Int J Nanomedicine*. 2012;7:2673–2685.
30. Arnida MA, Ghandehari H. Cellular uptake and toxicity of gold nanoparticles in prostate cancer cells: a comparative study of rods and spheres. *J Appl Toxicol*. 2010;30(3):212–217.
31. Wang SH, Lee CW, Chiou A, Wei PK. Size-dependent endocytosis of gold nanoparticles studied by three-dimensional mapping of plasmonic scattering images. *J Nanobiotechnology*. 2010;8:33.
32. Varela JA, Bexiga MG, Aberg C, Simpson JC, Dawson KA. Quantifying size-dependent interactions between fluorescently labeled polystyrene nanoparticles and mammalian cells. *J Nanobiotechnology*. 2012;10:39.
33. Huang J, Bu L, Xie J, et al. Effects of nanoparticle size on cellular uptake and liver MRI with polyvinylpyrrolidone-coated iron oxide nanoparticles. *ACS Nano*. 2010;4(12):7151–7160.
34. Gliga AR, Skoglund S, Wallinder IO, Fadeel B, Karlsson HL. Size-dependent cytotoxicity of silver nanoparticles in human lung cells: the role of cellular uptake, agglomeration and Ag release. *Part Fibre Toxicol*. 2014;11:11.
35. Chen LQ, Fang L, Ling J, Ding CZ, Kang B, Huang CZ. Nanotoxicity of silver nanoparticles to red blood cells: size dependent adsorption, uptake, and hemolytic activity. *Chem Res Toxicol*. 2015;28(3):501–509.
36. Canton I, Battaglia G. Endocytosis at the nanoscale. *Chem Soc Rev*. 2012;41(7):2718–2739.
37. Chithrani BD. Optimization of bio-nano interface using gold nanostructures as a model nanoparticle system. *Insci J*. 2011;1:115–135.
38. Chithrani BD, Stewart J, Allen C, Jaffray DA. Intracellular uptake, transport, and processing of nanostructures in cancer cells. *Nanomed*. 2009;5(2):118–127.
39. Milić M, Leitinger G, Pavičić I, et al. Cellular uptake and toxicity effects of silver nanoparticles in mammalian kidney cells. *J Appl Toxicol*. 2015;35(6):581–592.
40. Krpetic Z, Saleemi S, Prior IA, See V, Qureshi R, Brust M. Negotiation of intracellular membrane barriers by TAT-modified gold nanoparticles. *ACS Nano*. 2011;5(6):5195–5201.
41. Selby LI, Cortez-Jugo CM, Such GK, Johnston APR. The proton sponge: a trick to enter cells the viruses did not exploit. *Chim Int J Chem*. 1997;2:34–36.
42. Greulich C, Diendorf J, Simon T, Eggeler G, Epple M, Koller M. Uptake and intracellular distribution of silver nanoparticles in human mesenchymal stem cells. *Acta Biomater*. 2011;7(1):347–354.
43. Zuhorn IS, Kalicharan R, Hoekstra D. Lipoplex-mediated transfection of mammalian cells occurs through the cholesterol-dependent clathrin-mediated pathway of endocytosis. *J Biol Chem*. 2002;277(20):18021–18028.
44. Wang Z, Li N, Zhao J, White JC, Qu P, Xing B. CuO nanoparticle interaction with human epithelial cells: cellular uptake, location, export, and genotoxicity. *Chem Res Toxicol*. 2012;25(7):1512–1521.
45. Fahrenkrog B, Aebi U. The nuclear pore complex: nucleocytoplasmic transport and beyond. *Nat Rev Mol Cell Biol*. 2003;4(10):757–766.
46. Wente SR. Gatekeepers of the nucleus. *Science*. 2000;288(5470):1374–1377.

47. Dawson KA, Salvati A, Lynch I. Nanotoxicology: nanoparticles reconstruct lipids. *Nat Nanotechnol*. 2009;4(2):84–85.
48. Kang B, Mackey MA, El-Sayed MA. Nuclear targeting of gold nanoparticles in cancer cells induces DNA damage, causing cytokinesis arrest and apoptosis. *J Am Chem Soc*. 2010;132(5):1517–1519.
49. Kim HR, Kim MJ, Lee SY, Oh SM, Chung KH. Genotoxic effects of silver nanoparticles stimulated by oxidative stress in human normal bronchial epithelial (BEAS-2B) cells. *Mutat Res*. 2011;726(2):129–135.
50. Asharani PV, Hande MP, Valiyaveettil S. Anti-proliferative activity of silver nanoparticles. *BMC Cell Biol*. 2009;10(65):1–14.
51. Lu W, Senapati D, Wang S, et al. Effect of surface coating on the toxicity of silver nanomaterials on human skin keratinocytes. *Chem Phys Lett*. 2010;487(1–3):92–96.
52. Hackenberg S, Scherzed A, Kessler M, et al. Silver nanoparticles: evaluation of DNA damage, toxicity and functional impairment in human mesenchymal stem cells. *Toxicol Lett*. 2011;201(1):27–33.

Supplementary material

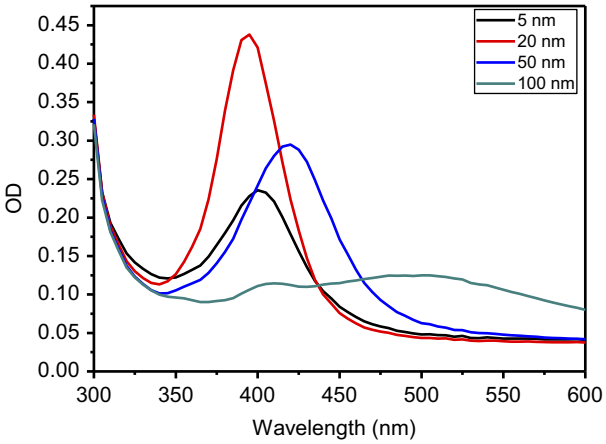

Figure S1 UV analysis of AgNPs at the concentration of 10 μg/mL.
Abbreviation: AgNPs, silver nanoparticles.

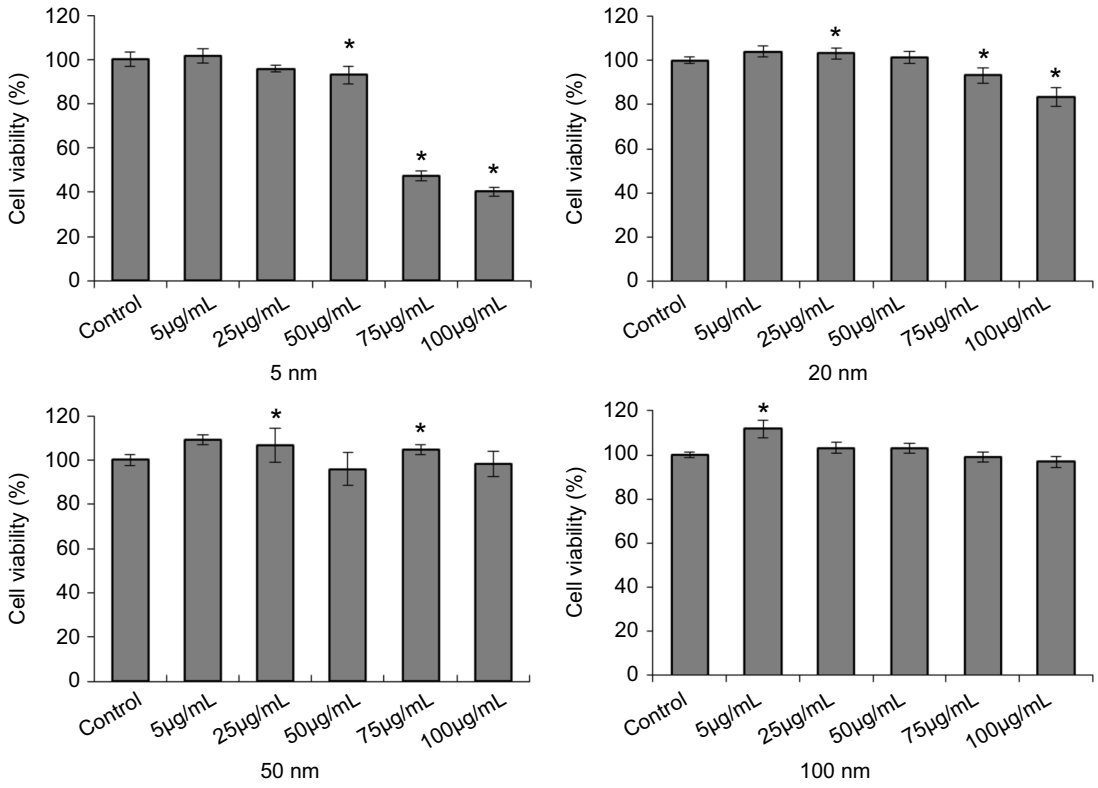

Figure S2 Cell viability of B16 cells with AgNPs treatment. After 24 hours incubation, cells were harvested and detatched by a MTS assay kit. This assay were performed three times, and representative results areshown here (Mean value±SD, n=4 for each group; *P<0.05, significantly different from the control.
Abbreviation: AgNPs, silver nanoparticles.

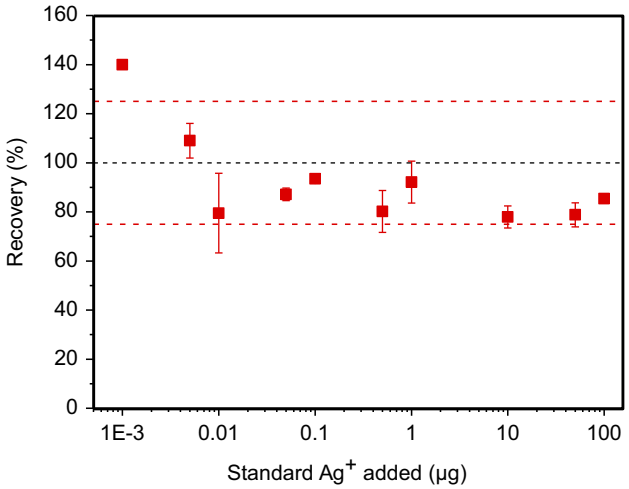

Figure S3 The recovery percentage of Ag by ICP-MS. Standard silver nitrate solutions containing 0.001–100 μg Ag were digested with microwave before ICP-MS measurement. The limit of detection of Ag was 0.003 μg by this method (n=3 for each group, black dashed line: 100% yield, red dashed line: 100±25%).
Abbreviations: Ag, silver; ICP-MS, inductively coupled plasma mass spectrometry.

International Journal of Nanomedicine

Dovepress

Publish your work in this journal

The International Journal of Nanomedicine is an international, peer-reviewed journal focusing on the application of nanotechnology in diagnostics, therapeutics, and drug delivery systems throughout the biomedical field. This journal is indexed on PubMed Central, MedLine, CAS, SciSearch®, Current Contents®/Clinical Medicine, Journal Citation Reports/Science Edition, EMBase, Scopus and the Elsevier Bibliographic databases. The manuscript management system is completely online and includes a very quick and fair peer-review system, which is all easy to use. Visit http://www.dovepress.com/testimonials.php to read real quotes from published authors.

Submit your manuscript here: https://www.dovepress.com/international-journal-of-nanomedicine-journal